ACS Catalysis

Letter

pubs.acs.org/acscatalysis

Ti-YNU-2: A Microporous Titanosilicate with Enhanced Catalytic Performance for Phenol Oxidation

Makiko Sasaki, Yuya Sato, Yasuyuki Tsuboi, Satoshi Inagaki, and Yoshihiro Kubota*

Division of Materials Science and Chemical Engineering, Yokohama National University, 79-5 Tokiwadai, Hodogaya-ku, Yokohama 240-8501, Japan

Supporting Information

ABSTRACT: YNU-2P, a highly crystalline composite of organic structure-directing agent and pure-silica MSE precursor, was stabilized by steaming so as to retain adequate site defects. To the remaining site defects, the efficient introduction of Ti into the framework was accomplished to give the new microporous titanosilicate Ti-YNU-2 after optimizing the conditions for steaming and vapor phase $TiCl_4$ treatments. This material proved to be a high-performance catalyst, exhibiting remarkably enhanced performance compared to Ti-MCM-68, a material already known to show superior performance to TS-1, during phenol oxidation using H_2O_2 as an oxidant.

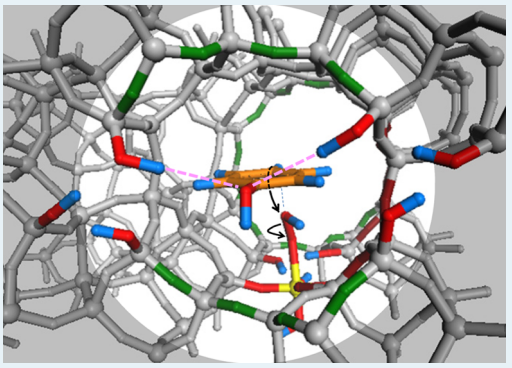

KEYWORDS: *YNU-2, MSE, MCM-68, defect, steaming, titanosilicate, phenol oxidation, hydrogen peroxide*

Microporous crystalline titanosilicates are highly efficient catalysts for the selective oxidation of a wide range of organic substrates using hydrogen peroxide (H_2O_2).[1−5] H_2O_2 represents a desirable oxidant for liquid phase reactions from an environmental point of view when compared with peracids (RCO_3H) or alkyl hydroperoxides (ROOH),[6] because it is able to oxidize organic compounds with an atom efficiency of 47% and with the generation of water as the only coproduct. Thus, the combined use of titanosilicates with H_2O_2 is a promising means of developing green, sustainable processes. To meet the requirements of various reactions and to take advantage of different zeolite structures, a variety of titanosilicates, including TS-1 (Ti-MFI),[7] TS-2 (Ti-MEL),[8] Ti-beta (Ti-BEA),[9−11] Ti-ZSM-12 (Ti-MTW),[12] Ti-ZSM-48,[13] Ti-mordenite (Ti-MOR),[14] Ti-SSZ-33,[15] Ti-ITQ-7 (Ti-ISV),[16] and Ti-MCM-22 (Ti-MWW),[17−19] have been prepared by hydrothermal synthesis (HTS), dry-gel conversion (DGC),[11,19] and postsynthetic isomorphous substitution.[14,15,17,18] It is well-known that TS-1 is an industrially useful titanosilicate and effective for processes such as propene epoxidation, phenol oxidation, and cyclohexanone ammoximation. Due to its 10-ring (10R) structure, however, the activity of this material during epoxidation is significantly reduced when the substrate is cyclohexene or bulkier olefins. In contrast, Ti-BEA, which has large 3-D 12R pores, exhibits higher activity than TS-1 when the substrate is cyclohexene. Wu et al. have reported the high activity of Ti-MWW and have also demonstrated a remarkable enhancement in its activity with bulkier olefins by postsynthetic delamination[20] or pillaring.[21] However, both Ti-BEA and Ti-MWW show poor activities during phenol oxidation.[22] In addition, mesoporous titanosilicates such as Ti-MCM-41, which contain numerous hydrophilic surface silanol groups, suffer from the serious disadvantage of Ti leaching during reactions.[5]

Hydrophobicity is a necessary bulk property for a highly efficient oxidation catalyst, while at the atomic level, it is believed necessary to have isolated tetrahedral Ti species in the zeolite framework. In the course of developing new titanosilicate catalysts, however, we have found several exceptions in which nontetrahedral Ti species are quite active. We report here some modifications to the accepted theory of titanosilicate chemistry and describe specific research objectives and outcomes.

MCM-68 (**MSE** topology[23]) was first synthesized by Mobil researchers.[24] This material represents a new type of multidimensional zeolite possessing a 12 × 10 × 10-ring (12 × 10 × 10R) pore system. In this material, a straight 12R channel intersects two independent tortuous 10R channels and, in addition, an 18 × 12R supercage is present that is accessible only through 10R channels.[25] The framework has eight distinct T-sites (Figure S1). Zeolites of this type exhibit unique acid-catalytic properties[26,27] and are potentially useful as catalysts for the alkylation of aromatics,[28−30] as well as for the production of propene by naphtha cracking.[31,32] Their use as hydrocarbon traps has also been reported.[33] In addition, titanium-substituted MCM-68 has demonstrated a performance superior to that of TS-1 for the oxidation of phenols with H_2O_2 as an oxidant.[22]

Received: June 9, 2014
Revised: June 28, 2014
Published: July 2, 2014

Originally, the synthesis of MCM-68 was possible only under hydrothermal conditions using *N,N,N′,N′*-tetraethylbicyclo-[2.2.2]oct-7-ene-2,3:5,6-dipyrrolidinium diiodide as the organic structure-directing agent (OSDA). The gel composition window for the successful crystallization of the pure MCM-68 is very narrow and the Si/Al ratio of the product is limited to the range of 9 to 12.[24,25] The synthesis also required a long crystallization period of more than 10 days. The alteration of the chemical composition of the product through the direct crystallization of a pure **MSE** phase is also challenging and gives other phases such as ***BEA**, **MTW**, or **MOR**. We have previously succeeded in overcoming this limitation by utilizing steam-assisted crystallization (SAC),[34] a DGC technique, with some postsynthetic modifications, including silylation[35] or Si migration by steaming,[36] to obtain a pure-silica version of the **MSE** (YNU-2).[35,36] In this case, the required crystallization period is approximately 5 days.

With regard to the aluminosilicate version, we have succeeded in the synthesis of an Al-rich **MSE**-type zeolite (YNU-3) with a Si/Al molar ratio of approximately 7, requiring a relatively short crystallization period of only 3 days, via the hydrothermal conversion of an **FAU**-type zeolite.[37] Very recently, we reported the crystallization of a pure **MSE** phase over a span of 48−60 h by a seed-assisted OSDA-free synthesis[38] based on the so-called "CBU hypothesis",[39] as well as the pioneering work by Xiao et al.,[40] and the subsequent stabilization/dealumination of this material to allow its application to the catalytic cracking of *n*-hexane.[38]

Conversely, in the case of the titanosilicate version, direct crystallization of Ti-MSE is still difficult by any of the methods noted above, which were found to be effective for aluminosilicates. One option for introducing a sufficient amount of Ti into the framework is the isomorphous substitution of conventional Al-MCM-68, and we already reported the successful synthesis of Ti-MCM-68 (one of the Ti-MSE analogues) by postsynthetic modification (dealumination by acid treatment followed by gas-phase Ti insertion using $TiCl_4$ as the Ti source) of Al-MCM-68 (Al-MSE).[22] Superiority of the Ti-MCM-68 over more conventional titanosilicates such as Ti-BEA and Ti-MWW is prominent, and unexpectedly poor activities of Ti-BEA and Ti-MWW in our reaction system have also been reported.[22] Another possible option for the preparation of Ti-MSE is the insertion of Ti into the site defects of the highly defective precursor YNU-2P.[35,36] In this case, incomplete but effective Si migration would be required for framework stabilization while keeping the vacant sites (i.e., site defects) to be filled with Ti atoms.

In keeping with the above, we report herein the synthesis of Ti-YNU-2 (another Ti-MSE analogue) by the successful postsynthetic modification (stabilization by steam treatment followed by gas-phase Ti insertion using $TiCl_4$ as the Ti source) of YNU-2P. We also detail its excellent catalytic performance for the oxidation (hydroxylation) of phenol (Scheme 1) using H_2O_2 as an oxidant and examine the causes of the activity and selectivity of this material.

The precursor material, YNU-2P, was synthesized by previously reported procedures. A new aspect of this synthesis, however, is that the ***BEA** phase appears at a very early stage of the crystallization, followed by transformation to the **MSE** phase. The YNU-2P, a composite of the OSDA and an incomplete **MSE** framework, did not retain the framework structure upon removal of the OSDA, due to the significant concentration of site defects (vacant sites).[35] Filling these

Scheme 1. Assumed Reaction Pathways of Phenol Oxidation with H_2O_2 over a Titanosilicate Catalyst

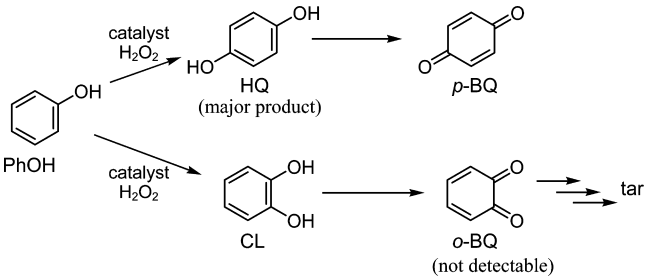

defects through steaming generated a more robust material[36] and steaming of the YNU-2P was carried out utilizing the equipment shown in Figure S2. Steam was supplied at various temperatures (t °C; 250−300 °C), and partial pressures (p kPa; 10−50 kPa) for 24 h and the resultant YNU-2 materials were denoted YNU-2(t, p), where t and p are the steam temperature in °C and the steam pressure in kPa, respectively. Within the range of these temperatures and pressures, steaming worked well for the stabilization of the **MSE** framework of YNU-2, although not at temperatures lower than 200 °C. The content of OSDA in the YNU-2P estimated by thermogravimetric analysis was 23 wt %; when p was 10, the organic contents were 21.1, 17.1, and 12.2 wt % after steaming at 200, 250, and 300 °C, respectively. It was thus suggested that the stabilization needs removal of adequate amount of organics (vide infra). From the stabilized samples, the remaining organics were completely removed after further calcination at 450 °C for 3 h without framework collapse. The ^{29}Si MAS NMR spectra (Figure S3) of the calcined products exhibited major Q^4 peaks and minor Q^3 peaks, indicating the presence of a stabilized framework as well as some remaining minor site defects. N_2 adsorption−desorption data showed significant hysteresis loops (Figures S4 b, c and e), suggesting the presence of mesopores as large as approximately 4 nm in YNU-2(250, 50), YNU-2(250, 30) and YNU-2(300, 30), which was confirmed by TEM observations of YNU-2(250, 30) (Figure S5). These results are consistent with the assumed Si migration we have already reported as the cause of the framework stabilization.[36,38] With regard to the framework stabilization induced by steaming, we speculate that the migration of $Si(OH)_4$ through the micropores takes place during the steam treatment from various regions within the crystal to the defect positions, and thus the site defects might be repaired by the condensation of $Si(OH)_4$ fragments.[36] The $Si(OH)_4$ migration may require some space generated by the adequate removal of organics from YNU-2P (vide supra). Slight changes in the steaming conditions were found to affect the subsequent Ti insertion into the framework and thus the catalytic performance of the resultant titanosilicate Ti-YNU-2. The Ti insertion was carried out according to the procedure carefully described in section 4 of Supporting Information utilizing the equipment shown in Figure S6.

Table 1 shows the results of phenol oxidation with H_2O_2 over Ti-YNU-2 catalysts prepared via different steaming conditions. Conventional Ti-MCM-68 and TS-1 were tested for comparison purposes. It should be noted that no interconversion was observed between hydroquinone (HQ) and catechol (CL) in independent experiments. The TON values exhibit a general tendency such that higher values are obtained at a steaming temperature of 250 °C as compared to 300 °C, whereas the optimal steaming pressure is as low as 10

dx.doi.org/10.1021/cs5007926 | ACS Catal. 2014, 4, 2653−2657

Table 1. Oxidation of Phenol with H_2O_2 over Various Titanosilicate Catalyst[a]

				yield[e] (%)					H_2O_2	
entry	catalyst[b]	Ti-content[c]/ mmol (g-cat.)$^{-1}$	TON[d]	total	HQ	CL	*p*-BQ	*para*-sel.[f] (%)	conv. (%)	eff.[g] (%)
1	Ti-YNU-2(250, 10)	0.18	923	74.3	58.4	6.1	9.8	92	88.4	83.2
2	Ti-YNU-2(250, 30)	0.16	786	59.2	45.2	7.4	6.7	88	82.9	71.5
3	Ti-YNU-2(250, 50)	0.16	704	53.0	38.4	6.5	8.1	88	90.3	58.7
4	Ti-YNU-2(300, 10)	0.20	444	42.2	27.5	4.6	10.1	89	67.8	62.2
5	Ti-YNU-2(300, 30)	0.10	127	5.7	2.6	1.4	1.7	76	20.1	28.2
6	Ti-YNU-2(300,50)	0.07	118	4.1	1.5	1.0	1.7	76	14.2	29.1
7	Ti-MCM-68-cal	0.25	272	32.3	22.2	8.3	1.8	74	63.3	51.1
8	Ti-MCM-68	0.25	150	17.1	11.1	5.5	0.5	58	34.0	50.1
9	TS-1	0.36	50	8.4	4.7	3.7	0.0	56	25.2	33.4

[a]Reaction conditions: phenol (PhOH), 21.05−21.85 mmol; catalyst, 20 mg; H_2O_2, 4.12−4.55 mmol; temperature, 100 °C; time, 10 min. [b]First and second values in parentheses are steaming temperature, *t*/°C, and steam pressure, *p*/kPa, respectively. [c]Determined by ICP analysis. [d]Turnover number (moles of [hydroquinone (HQ) + catechol (CL) + *p*-benzoquinone (*p*-BQ)] per mole of Ti site). [e]Product yields based on added H_2O_2 after exhaustive acetylation of the products with excess $(CH_3CO)_2O$-K_2CO_3, the derivatized products were analyzed by GC (0.25 mm × 30 m × 1.00 μm DB-1 column; internal standard: anisole; detector: FID). [f]Selectivity to *para*-isomers of dihydroxybenzenes and quinones (moles of [HQ + *p*-BQ] per moles of [HQ + CL + *p*-BQ]. [g]Efficiency of H_2O_2 utilization (moles of [HQ + CL + *p*-BQ] per mole of H_2O_2 converted).

kPa (entries 1−6). Careful screening confirmed the optimal steam temperature and pressure values as 250 °C and 10 kPa, respectively. Under these optimized conditions, significantly high values of TON, yield, and *para*-selectivity were obtained (entry 1) in the case of Ti-YNU-2 as compared to the results obtained with conventional Ti-MCM-68 (entries 7, 8). The much higher activity observed for Ti-MCM-68 compared to that seen with TS-1 (entry 9) may occur primarily because the 12R channel of the MSE framework is well-suited to the diffusion of molecules with a single aromatic ring, based on the assistance of the intersecting 10Rs.[22] Although calcination after the Ti introduction significantly improved the catalytic performance of Ti-MCM-68 (entry 7; Ti-MCM-68-cal vs entry 8) as a result of the associated increase in hydrophobicity,[22] Ti-YNU-2(250, 10) still shows far better catalytic performance than Ti-MCM-68-cal. Comparison of water adsorption isotherms at 25 °C between Ti-YNU-2(250, 10) and Ti-MCM-68-cal indicated that Ti-YNU-2(250, 10) adsorbs more water at $P/P_0 > 0.4$, whereas a comparative amount of water is adsorbed at $P/P_0 < 0.4$ (Figure S7a and S7d). On the ^{29}Si MAS NMR spectra of Ti-MCM-68-cal, slightly less Q^3 signals were observed compared with Ti-YNU-2(250, 10), as shown in Figure S8a and S3c. The ^{29}Si MAS NMR spectra of other titanosilicates included in Table 1 are shown with Q^3:Q^4 ratios in Figure S8b and S8c. Note that these characterizations may reflect the total hydrophilicity or total amount of Q^3 in the bulk material and not the local situation at a molecular level. The slightly more hydrophilic character of the Ti-YNU-2(250, 10) is due to the presence of relatively larger amount of defects (i.e., silanols); however, a hydrophobic area that can interact with aromatic moieties should still exist inside the micropore.

To determine why Ti-YNU-2 is so active, both the ground state and active modes of TS-1, Ti-MCM-68, and Ti-YNU-2 were examined by diffuse reflectance (DR) UV−vis spectroscopy, utilizing a pseudo-in situ cell.[41] Figure 1A shows the UV−vis spectra of TS-1, Ti-MCM-68, and Ti-YNU-2 under ambient conditions. The peaks at around 210 nm found in the spectra of all the titanosilicates are assignable to 4-coordinated "closed" and "open" Ti species.[4] However, a shoulder peak was observed at around 250−290 nm only in the case of Ti-YNU-2. Since peaks in this range are assigned to 5- or 6-coordinated Ti species,[4] the coordination states of the Ti-sites are evidently quite different in this material compared to those in TS-1 and Ti-MCM-68.

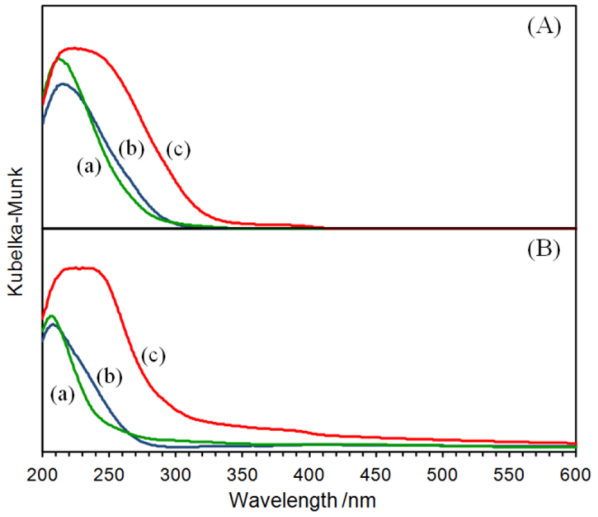

Figure 1. DR UV−vis spectra of various titanosilicate catalysts (A) before and (B) after evacuation taken by using a pseudo-in situ cell. Samples are (a) TS-1, (b) Ti-MCM-68, and (c) Ti-YNU-2. Evacuation was carried out at 400 °C for 2 h.

Figure 1B presents the DR UV−vis spectra obtained after evacuation at 400 °C for 2 h, using the pseudo-in situ cell.[41] The peaks for TS-1 and Ti-MCM-68 at around 210 nm became sharper after evacuation to give spectra more typical of 4-coordinated Ti-species, likely because the effect of adsorbed water was eliminated. In the case of the Ti-YNU-2, however, the second group of peaks (250−290 nm) was still prominent, indicating that it retained a relatively large amount of 5- or 6-coordinated Ti-species.[4] The coexistence of 4-coordinated Ti-species was also evident, and the presence of open sites with one or more hydroxy groups connected to a Ti atom was suggested, according to the literature reports concerning TS-1.[4]

According to the procedure described in Supporting Information, H_2O was added to the evacuated samples in the in situ cell, and DR UV−vis spectral data were collected to give the spectra shown in Figure 2A. The spectra obtained for TS-1 and Ti-MCM-68 were similar to that of Figure 1B(c), and were indicative of an increase in 5- or 6-coordinated Ti-species and/

dx.doi.org/10.1021/cs5007926 | ACS Catal. 2014, 4, 2653−2657

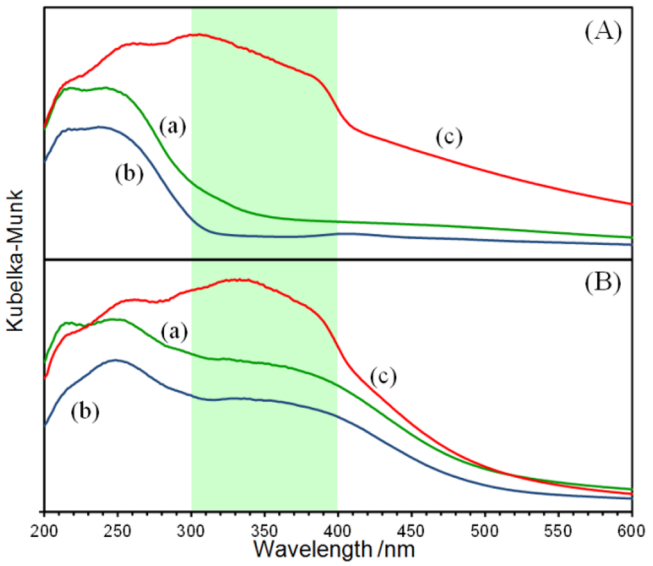

Figure 2. DR UV−vis spectra of various titanosilicate catalysts taken by using a pseudo-in situ cell after addition of (A) H_2O or (B) 31% aqueous solution of H_2O_2 to the evacuated samples as in Figure 2B. Samples are (a) TS-1, (b) Ti-MCM-68, and (c) Ti-YNU-2.

or 4-coordinated Ti with open sites. In contrast, the spectrum of Ti-YNU-2 had a totally different pattern (Figure 2A(c)), including a large, broad peak in the range of 300−400 nm (the pale green region in Figure 2) assignable to a 5- or 6-coordinated Ti-species with one or more hydroxy groups attached. Peaks in this region (300−400 nm) appeared for all samples when 31% H_2O_2/H_2O was added to the evacuated samples instead of pure H_2O, although the peak was particularly large in the case of Ti-YNU-2. The broad peaks in this region correspond to the Ti-OOH species associated with the working state of the titanosilicate catalysts. These findings suggest that Ti-YNU-2 has a much greater tendency to generate active Ti-OOH species than do TS-1 and Ti-MCM-68, and this could explain the remarkably enhanced activity of Ti-YNU-2.

Regarding the *para*-selectivity issue, the superiority of Ti-MCM-68 over TS-1 may be explained based on the fact that there is no large cavity at the 12/10R intersection, which may contribute to its high *para*-selectivity during phenol oxidation. In sharp contrast, TS-1 shows low activity and almost no *para*-selectivity, meaning that the reaction must take place at active sites on the external surface under the current reaction conditions.[22]

The reason why Ti-YNU-2 is so *para*-selective may be explained as follows. According to our previous reports,[35,36] the precursor YNU-2P has significant site defects at the T6 and T7 sites (T7 and T8 in ref 23, respectively). These sites do not face the 12R channel of the **MSE** framework. We therefore speculate that, with the aid of steaming, the Si atoms migrate from T3 and T5 sites to adjacent defects at T6 and T7, respectively, to fill up these sites, resulting in the possible formation of new defects at T3 and T5 that face 12R. Now the insertion of Ti at the T3 and/or T5 sites is possible and this could account for the presence of active sites at the 12R position. Incomplete connectivity around the Ti may also allow changes in both the coordination number and the structure of the Ti complex moiety. Such kind of Ti site located near a silicon vacancy terminated with hydrogen atoms forming a silanol nest has been assumed in the framework of TS-1 and formation of distorted octahedral Ti complex within the framework was suggested by an electronic density functional theory (DFT) methods.[42] Figure 3 illustrates the Ti atom at a

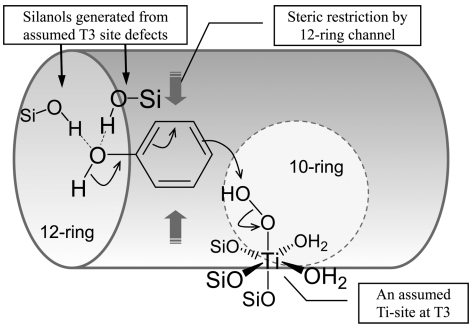

Figure 3. Schematic illustration showing possible interactions between a phenol molecule and an active-state framework of Ti-YNU-2 including a Ti-OOH site and other site defects. The curly arrows are so-called "arrow pushing" illustrating the movement of electrons as bonds are cleaved and new bonds or charges are formed. More exact positioning is shown in Supporting Information Figure S9.

T3 site coordinated with OOH and the presence of Si−OH generated by the remaining site defect at another T3. The Si−OH groups at the second and third T3 sites may have a positioning effect on the phenol molecule via hydrogen bonding (as could another T5 site), making the *para*-position reactive with the oxygen of the TiOOH group at the proximate T3 site. In this manner, the oxidation proceeds not simply by classic shape-selectivity[43] but rather by a more sophisticated transition state which could occur with the aid of an interaction between the phenolic OH and Si−OH groups at particular site defects. More detailed visualization of the possible interactions between a phenol molecule and an active-state framework of Ti-YNU-2 is displayed in Figure S9. With regard to practicality, the Ti-YNU-2 was reusable at least once with maintaining the high level of selectivity and with no decrease in activity (Table S1). The spent catalyst was regenerated before next use by washing with water and calcination at 550 °C for 4 h. Although the decrease to a certain extent in activity was detected at the third run (second reuse), Ti-leaching was not obvious after second run (first reuse) as confirmed by the elemental analysis of the spent catalysts (Table S1). This material thus shows promise for the development of new green chemical processes. Reusability was more excellent for TS-1; however, intrinsic selectivity and activity of the TS-1 for this reaction were moderate (Table S1).

In summary, a new type of microporous titanosilicate, Ti-YNU-2, was prepared by postsynthetic stabilization of the highly defective precursor YNU-2P based on Si migration during steam treatment under relatively mild conditions, followed by vapor-phase $TiCl_4$ treatment. The Ti-YNU-2 exhibited far superior activity and selectivity than the conventional Ti-MCM-68 catalyst, which in turn shows superior performance to TS-1 for phenol oxidation when using H_2O_2 as an oxidant. The high activity and *para*-selective nature of the Ti-MSE materials (Ti-MCM-68 and Ti-YNU-2) were ascribed to elevated diffusivity in the 12R channel compared to that in the 10R channels as well as the absence of a large cavity at 12/10R intersections, respectively. Besides these common factors, Ti-YNU-2 exhibited a significantly different character. The relatively large amount of site defects at

dx.doi.org/10.1021/cs5007926 | *ACS Catal.* 2014, 4, 2653−2657

specific T sites in this material may promote the formation of a more defined transition state than the classical size-restriction mechanism[43] based on simple confinement. This suggests that a defined transition state, possibly involving interaction between a metal−complex catalyst and an organic substrate, could operate in zeolite micropores. This finding could lead to a new generation of catalyst design based on microporous titanosilicates.

■ ASSOCIATED CONTENT

Supporting Information

Further details concerning the experimental procedures as well as the results of catalyst reuse, a drawing of T-sites, illustrations of equipment for steaming and Ti-insertion, ^{29}Si MAS NMR of various titanosilicates, N_2 adsorption isotherms, a TEM image, water adsorption isotherms, and a graphic of the possible interactions between a phenol molecule and an active-state framework of Ti-YNU-2 are included in Supporting Information. This material is available free of charge via the Internet at http://pubs.acs.org.

■ AUTHOR INFORMATION

Corresponding Author

*E-mail: kubota@ynu.ac.jp.

Notes

The authors declare no competing financial interest.

■ ACKNOWLEDGMENTS

This study was financially supported in part by Grant-in-Aid for Scientific Research (nos. 13199071 and 23760741). We acknowledge Dr. K. Yoshida and Dr. Y. Sasaki of Japan Fine Ceramics Center (JFCC) for TEM observation. The authors also thank Professor T. Tatsumi of Tokyo Institute of Technology and Mr. Yuji Nishita of Yokohama National University for helpful discussion and technical assistance, respectively.

■ REFERENCES

(1) Notari, B. *Adv. Catal.* **1996**, *41*, 253−334.
(2) Tatsumi, T. *Curr. Opin. Solid State Mater. Sci.* **1997**, *2*, 76−83.
(3) Arends, I. W. C. E.; Sheldon, R. A. *Appl. Catal., A* **2001**, *212*, 175−187.
(4) Ratnasamy, P.; Srinivas, D.; Knoezinger, H. *Adv. Catal.* **2004**, *48*, 1−169.
(5) Wu, P.; Tatsumi, T. *Catal. Surv. Asia* **2004**, *8*, 137−148.
(6) Noyori, R.; Aoki, M.; Sato, K. *Chem. Commun.* **2003**, *39*, 1977−1986.
(7) Taramasso, M.; Perego, G.; Notari, B. U.S. Patent No. 4,410,501, October 18, 1983.
(8) Reddy, J. S.; Kumar, R.; Ratnasamy, P. *Appl. Catal.* **1990**, *58*, L1−L3.
(9) Camblor, M. A.; Corma, A.; Martínez, A.; Pérez-Pariente, J. *J. Chem. Soc., Chem. Commun.* **1992**, *28*, 589−590.
(10) Inagaki, S.; Takechi, K.; Kubota, Y. *Chem. Commun.* **2010**, *46*, 2662−2664.
(11) Tatsumi, T.; Jappar, N. *J. Phys. Chem. B* **1998**, *102*, 7126−7131.
(12) Tuel, A. *Zeolites* **1995**, *15*, 236−242.
(13) Serrano, D. P.; Li, H.-X.; Davis, M. E. *J. Chem. Soc., Chem. Commun.* **1992**, *28*, 745−747.
(14) Wu, P.; Komatsu, T.; Yashima, T. *J. Phys. Chem.* **1996**, *100*, 10316−10322.
(15) Dartt, C. B.; Davis, M. E. *Appl. Catal., A* **1996**, *143*, 53−73.
(16) Díaz-Cabañas, M.-J.; Villaescusa, L. A.; Camblor, M. A. *Chem. Commun.* **2000**, *36*, 761−762.
(17) Wu, P.; Tatsumi, T.; Komatsu, T.; Yashima, T. *J. Phys. Chem. B* **2001**, *105*, 2897−2905.
(18) Wu, P.; Tatsumi, T. *Chem. Commun.* **2002**, *38*, 1026−1027.
(19) Wu, P.; Miyaji, T.; Liu, Y.; He, M.; Tatsumi, T. *Catal. Today* **2005**, *99*, 233−240.
(20) Wu, P.; Nuntasri, D.; Ruan, J.; Liu, Y.; He, M.; Fan, W.; Terasaki, O.; Tatsumi, T. *J. Phys. Chem. B* **2004**, *108*, 19126−19131.
(21) Fan, W.; Wu, P.; Namba, S.; Tatsumi, T. *Angew. Chem., Int. Ed.* **2003**, *43*, 236−240.
(22) Kubota, Y.; Koyama, Y.; Yamada, T.; Inagaki, S.; Tatsumi, T. *Chem. Commun.* **2008**, *44*, 6224−6226.
(23) Baerlocher, Ch.; McCusker, L. B.; Olson, D. H. *Atlas of Zeolite Framework Types*, 6th ed.; Elsevier: Amsterdam, 2007; see also: http://www.iza-structure.org/databases/.
(24) Calabro, D. C.; Cheng, J. C.; Crane Jr, R. A.; Kresge, C. T.; Dhingra, S. S.; Steckel, M. A.; Stern, D. L.; Weston, S. C. U.S. Patent No. 6,049,018, 2000.
(25) Dorset, D. L.; Weston, S. C.; Dhingra, S. S. *J. Phys. Chem. B* **2006**, *110*, 2045−2050.
(26) Žilková, N.; Bejblová, M.; Gil, B.; Zones, S. I.; Burton, A. W.; Chen, C.-Y.; Musilová-Pavlačková, M.; Košová, G.; Čejka, J. *J. Catal.* **2009**, *266*, 79−91.
(27) Gil, B.; Košová, G.; Čejka, J. *Microporous Mesoporous Mater.* **2010**, *129*, 256−266.
(28) Shibata, T.; Suzuki, S.; Kawagoe, H.; Komura, K.; Kubota, Y.; Sugi, Y.; Kim, J.-H.; Seo, G. *Microporous Mesoporous Mater.* **2008**, *116*, 216−226.
(29) Shibata, T.; Kawagoe, H.; Naiki, H.; Komura, K.; Kubota, Y.; Sugi, Y. *J. Mol. Catal. A: Chem.* **2009**, *297*, 80−85.
(30) Ernst, S.; Elangovan, S. P.; Gerstner, M.; Hartmann, M.; Sauerbeck, S. *Abstr 14th Int. Zeol. Conf.* **2004**, 982.
(31) Inagaki, S.; Takechi, K.; Kubota, Y. *Chem. Commun.* **2010**, *46*, 2662−2664.
(32) Kubota, Y.; Inagaki, S.; Takechi, K. *Catal. Today* **2014**, *226*, 109−116.
(33) Elangovan, S. P.; Ogura, M.; Ernst, S.; Hartmann, M.; Tontisirin, S.; Davis, M. E.; Okubo, T. *Microporous Mesoporous Mater.* **2006**, *96*, 210−215.
(34) Matsukata, M.; Ogura, M.; Osaki, T.; Rao, P. R. H. P.; Nomura, M.; Kikuchi, E. *Top. Catal.* **1999**, *9*, 77−92.
(35) Koyama, Y.; Ikeda, T.; Tatsumi, T.; Kubota, Y. *Angew. Chem., Int. Ed.* **2008**, *47*, 1042−1046.
(36) Ikeda, T.; Inagaki, S.; Hanaoka, T.; Kubota, Y. *J. Phys. Chem. C* **2010**, *114*, 19641−19648.
(37) Inagaki, S.; Tsuboi, Y.; Nishita, Y.; Syahylah, T.; Wakihara, T.; Kubota, Y. *Chem.—Eur. J.* **2013**, *19*, 7780−7786.
(38) Kubota, Y.; Itabashi, K.; Inagaki, S.; Nishita, Y.; Komatsu, R.; Tsuboi, Y.; Shinoda, S.; Okubo, T. *Chem. Mater.* **2014**, *26*, 1250−1259.
(39) Itabashi, K.; Kamimura, Y.; Iyoki, K.; Shimojima, A.; Okubo, T. *J. Am. Chem. Soc.* **2012**, *134*, 11542−11549.
(40) Xie, B.; Song, J.; Ren, L.; Ji, Y.; Li, J.; Xiao, F.-S. *Chem. Mater.* **2008**, *20*, 4533−4535.
(41) Zecchina, A.; Bordiga, S.; Lamberti, C.; Ricchiardi, G.; Lamberti, C.; Ricchiardi, G.; Scarano, D.; Petrini, G.; Leofanti, G.; Mantegazza, M. *Catal. Today* **1996**, *32*, 97−106.
(42) Wells, D. H., Jr.; Delgass, W. N.; Thomson, K. T. *J. Am. Chem. Soc.* **2004**, *126*, 2956−2962.
(43) Csicsery, S. M. *Pure Appl. Chem.* **1986**, *58*, 841−856.